

Development and evaluation of a Venus flytrap-inspired microrobot

Liwei Shi¹ · Shuxiang Guo¹

Received: 12 February 2015 / Accepted: 3 March 2015
© Springer-Verlag Berlin Heidelberg 2015

Abstract Nature has provided the inspiration for many robots, leading to the development of biomimetic machines based on stick insects, jellyfish, butterflies, lobsters, and inchworms. Some carnivorous plants are capable of rapid motion, including mimosa, Venus flytraps, telegraph plants, sundews, and bladderworts, all of which are of interest in the design of biomimetic robots that can be activated in a controlled manner to capture prey using trigger hairs. Here, we describe a biomimetic robotic inspired by a Venus flytrap and fabricated using two ionic polymer metal composite (IPMC) actuators. First, we describe the structure of the robotic flytrap, which consists of two IPMC lobes and a proximity sensor, and discuss the design of the control circuitry. We then evaluate the deformation and bending force of the IPMC actuator with various applied signal voltages. We describe a prototype robotic flytrap utilising a proximity sensor to imitate the trigger hairs of the Venus flytrap. We conducted an experiment to assess the feasibility of the biomimetic flytrap. To evaluate grasping ability, we measured the maximum grasping payload with different applied voltages. To enlarge the working area, we integrated biomimetic walking and rotating motion into the robotic Venus flytrap. This paper describes a prototype movable robotic Venus flytrap and evaluates its walking and rotating speeds.

1 Introduction

Over the course of evolutionary history, diverse locomotive strategies have emerged in nature: swimming, rowing, flapping, floating, and sinking motions in water; crawling, walking, climbing, jumping, and rolling motions on land; and flying, gliding, and wafting motions in air. Furthermore, assisting actions such as sucking, clasping, ejecting, and grasping, are often employed to improve the efficiency of these locomotive strategies (Behkam and Sitti 2006; Yim et al. 2007; Shi et al. 2011, 2012; Zhang et al. 2006). The abundant structures in nature have inspired the design of biomimetic robots; however, the structure of conventional electromagnetic motors is not straightforward to miniaturise, and complex shapes are not easy to implement. Electric motors are therefore rarely used in such applications, and more novel actuator materials are more commonly used (Behkam and Sitti 2006; Liu et al. 2010). A variety of smart materials have been investigated for use as artificial muscles in biomimetic robots, including ionic polymer metal composites (IPMCs), piezoelectric elements, pneumatic actuators, and shape memory alloys (Heo et al. 2007; Wang et al. 2008; Villanueva et al. 2010, 2011; Chu et al. 2012; Kim et al. 2005).

Some carnivorous plants are capable of rapid movement, which is commonly exploited to trap invertebrates, small frogs, or mammals. The Venus flytrap lures prey via a sweet nectar. Once the prey moves trigger hairs, an action potential is generated, which propagates across a pair of lobes, stimulating it to implement rapid closing of the trap.

In summer months, many flying insects can act as vectors for malaria, dengue, West Nile virus, yellow fever, encephalitis, and other infectious diseases. A robotic flytrap could potentially be used to control the number of flying insects. Shahinpoor et al. developed a robotic Venus flytrap

✉ Liwei Shi
shiliwei@bit.edu.cn

¹ School of Life Science, Beijing Institute of Technology, Haidian District, Beijing 100081, China

using two IPMC lobes and four IPMC bristles (Shahinpoor 2011), but the output of the IPMC bristles used as trigger hairs was weak and unstable. Furthermore, the bending of the bristles was limited to two directions, which may fail to detect the presence of a fly when it pushes the bristles in an insensitive direction. Moreover, their robotic Venus flytrap was fixed, which may limit its applications.

In this work, we used IPMC as an actuator material to develop a robotic flytrap. We used a short-range proximity sensor to detect a fly or other moving object between the two IPMC lobes, and measured the maximum grasping payload with different applied voltages to evaluate its grasping ability. To enlarge the working area, we integrated biomimetic walking and rotating motion into the robotic Venus flytrap. We developed a prototype motile robotic Venus flytrap, and evaluated its walking and rotating speeds. The robotic flytrap performed well, mimicking the behaviour of the Venus flytrap found in nature, which demonstrates its potential for outdoor applications in capturing flies. We applied three lobes and three proximity sensors to improve the structure to reduce the gaps. The resulting prototype robotic flytrap was shown to be feasible in detecting and grasping flying insects and was driven using a low voltage, making it both electrically safe and economical and demonstrating its potential for applications such as toys or use in aquaria.

The remainder of this paper is divided into six parts. First, we describe the structure of the robotic flytrap. Second, we describe the deflection and bending force of the IPMC actuators. Third, we discuss the design of the robotic flytrap and the development of a prototype body, together with a series of experiments to evaluate the detection stability and trapping ability. Fourth, we describe the movable structure of the robotic flytrap and evaluate its walking and rotating ability. Fifth, we discuss an improved body structure of the robotic flytrap using three lobes. Finally, we present our conclusions.

2 The robotic Venus flytrap

2.1 Body structure

The Venus flytrap is one of a small group of plants that is capable of rapid movement. It consists of two lobes and several trigger hairs, as shown in Fig. 1. When the trigger hairs are stimulated, an action potential is generated, and the two lobes are stimulated to close quickly (http://en.wikipedia.org/wiki/Venus_Flytrap). Here, we propose a biomimetic robotic flytrap, as shown in Fig. 2. It uses two IPMC actuators to form a pair of lobes. The dimensions of the IPMC actuators were $24 \times 18 \times 0.22 \text{ mm}^3$, and the chamfer radius was 8 mm. The separation between the two

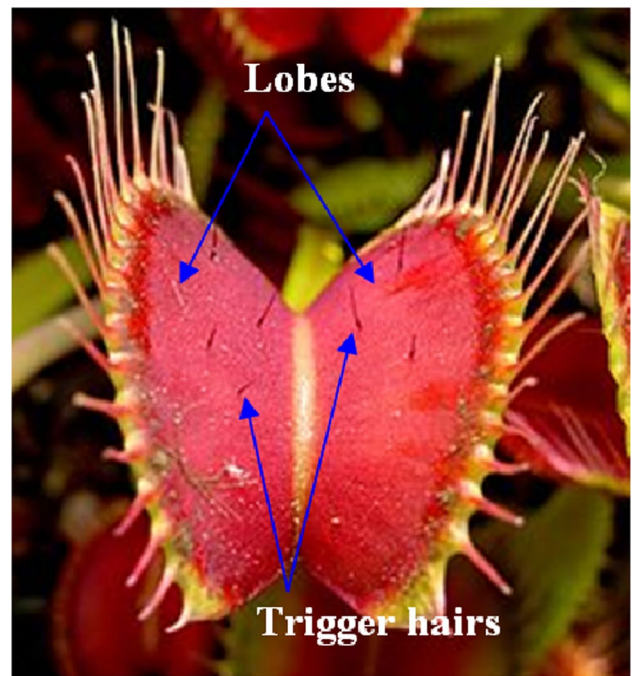


Fig. 1 A Venus flytrap (http://en.wikipedia.org/wiki/Venus_Flytrap)

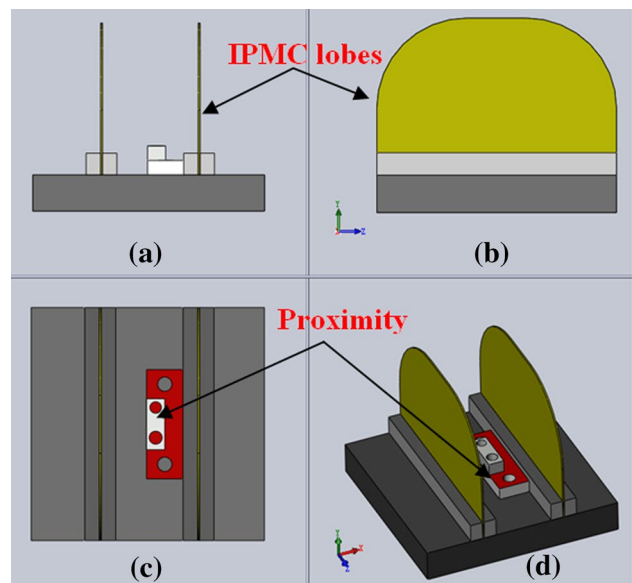
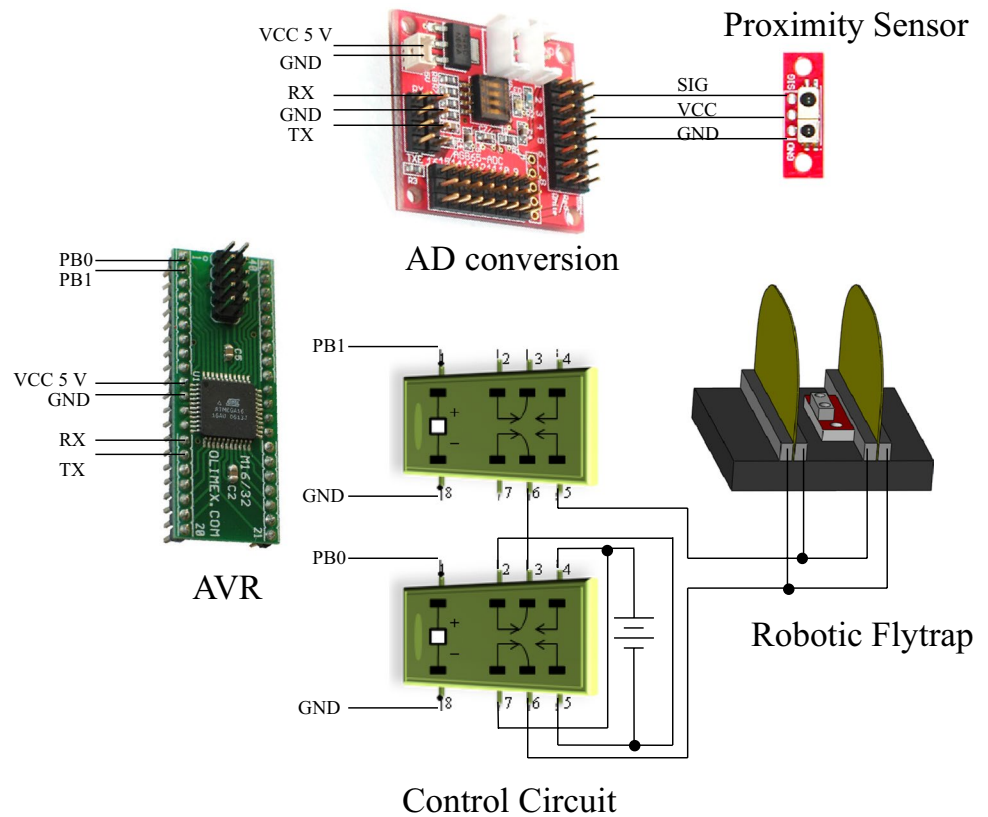


Fig. 2 Structure of the proposed robotic Venus flytrap

IPMC lobes was adjustable. We used an infrared proximity sensor to imitate the trigger hairs of the Venus flytrap, and calibrated the sensor to determine the distance between the sensor and the fly. The infrared proximity sensors used here were 10 mm long and 5 mm wide, with a mass of 0.7 g. The angle measurement for the proximity sensor ranged from -30° to 30° , which was sufficient to monitor the region between the two IPMC lobes.

Fig. 3 Control circuit used for the robotic flytrap



2.2 Control circuitry

Figure 3 shows the control circuit of the robotic flytrap. We used an AVR microcontroller as the control centre, with two electric relays to control the signal voltages of the IPMC lobes. The measurement range for one sensor was 0–60 mm, and the output voltage ranged from 150 mV to 5 V (Guo et al. 2012).

We calibrated the proximity sensor to determine the separation between the sensor and the fly. When the distance separation changed from 60 to 25 mm, the output voltage increased slowly from 0 to 0.2 V; when the separation was less than 25 mm, the output voltage increased rapidly. Based on these calibration results, we set the threshold voltage to obtain a threshold separation between the sensor and the fly corresponding to the space between the two lobes.

3 Analysis of the IPMC actuator

The IPMC actuator was formed of an ionic polymer membrane plated with gold electrodes on both sides (Shi et al. 2013). When a voltage is applied across the membrane, bending deformation of the IPMC actuator occurs, which results from a redistribution of the internal water molecules (Shi et al. 2012). IPMC exhibits a rapid response time, a

large bending deformation, and is compact, lightweight, and soft; furthermore, it requires low driving power, is low-noise, and can have a long service life (Park et al. 2007; Kim et al. 2011; Feng and Liu 2014). Wei and Su 2012 Due to these characteristics, IPMC actuators have been widely used in soft robotic structures, including artificial muscles, as well as in dynamic sensors (Kim et al. 2005; Shahinpoor 2011; Jain et al. 2011; Lee et al. 2007; Brunetto et al. 2008; Yeom and Oh 2009).

We used 220- μ m-thick Nafion™ 117 films, with Au thin films deposited on either side. These IPMC actuators can be considered as equivalent cantilever beams (Lin et al. 2014; He et al. 2011; Zhou et al. 2013). To investigate the bending performance, we clamped one end of the IPMC membrane, applied a voltage across the membrane, and measured the deflection of the free end in a water tank as a function of the applied voltage signal (Shi et al. 2013a). We found that the displacement of the tip decreased as the frequency of the voltage signal increased. We also measured the bending force generated at the free end of the equivalent cantilever with different applied voltage signals. The sample IPMC actuator was 24 mm long, 18 mm wide, and 220 μ m thick (the same dimensions as the lobes of the biomimetic flytrap). A signal was created using a PC equipped with a digital-to-analogue converter card, and the bending force of the IPMC was measured using an electronic

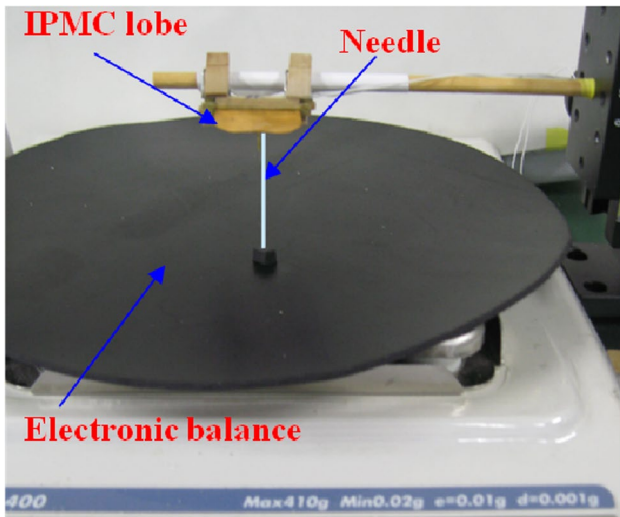


Fig. 4 Experimental system used to evaluate the bending force of the biomimetic actuators

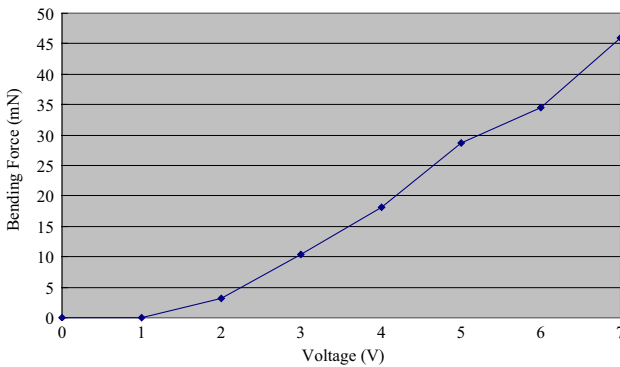


Fig. 5 Bending force of the IPMC actuator

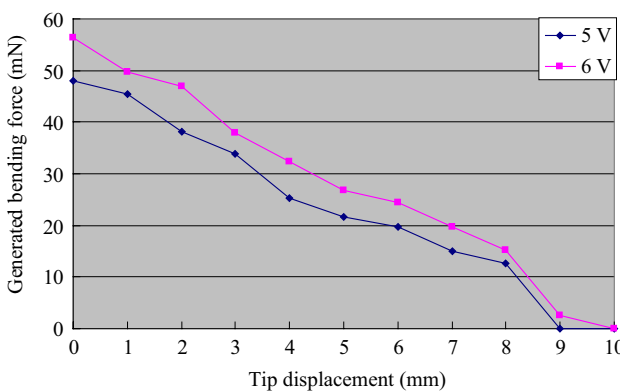


Fig. 6 Bending force of the IPMC actuator with various displacements

balance, as shown in Fig. 4. Figure 5 shows the measured bending force at the tip as a function of the applied voltage. To reduce the torque on the electronic balance, we used a perpendicular fixed needle to transfer the force from the actuator to the electronic balance. To eliminate the pretightening force between the IPMC and the needle, we set the initial distance between the IPMC and the needle tip to 3.5 mm. The results revealed that the bending force at the tip increased as the applied voltage increased: the maximum force was 45 mN with a voltage of 7 V.

The bending force of the IPMC actuator was also determined by the tip displacement. We measured the bending forces at the free end of the actuator with various initial distances between the IPMC and the tip of the needle, as shown in Fig. 6. The bending force of the IPMC actuator decreased when the tip displacement increased.

4 Prototype robotic flytrap

4.1 Prototype

Figure 7 shows the prototype robotic flytrap, which consisted of two IPMC lobes and an infrared sensor. It was 45 mm long, 40 mm wide, and 32 mm high, and weighed 6.252 g. The IPMC actuators were attached using copper clips, which also functioned as electrodes (Shi et al. 2012, 2013). The separation between the two IPMC lobes was 10 mm, and the control signals were transmitted via enamel-coated wires from the control circuit.

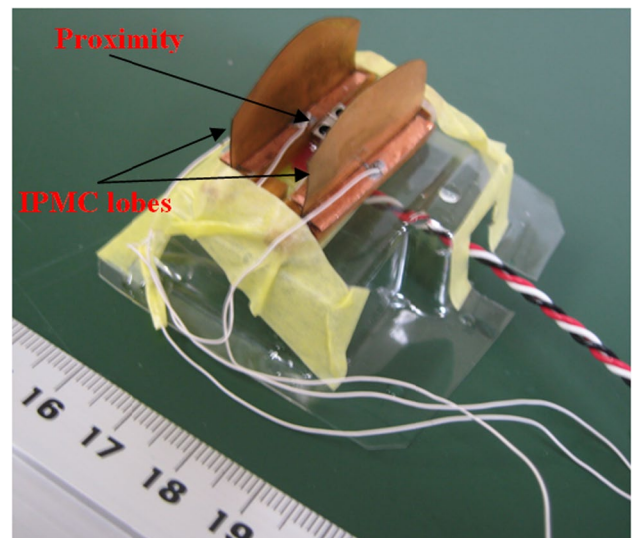


Fig. 7 The prototype robotic flytrap

Fig. 8 Closing motion without the sensor: **a** initial state and **b** maximum closing deformation

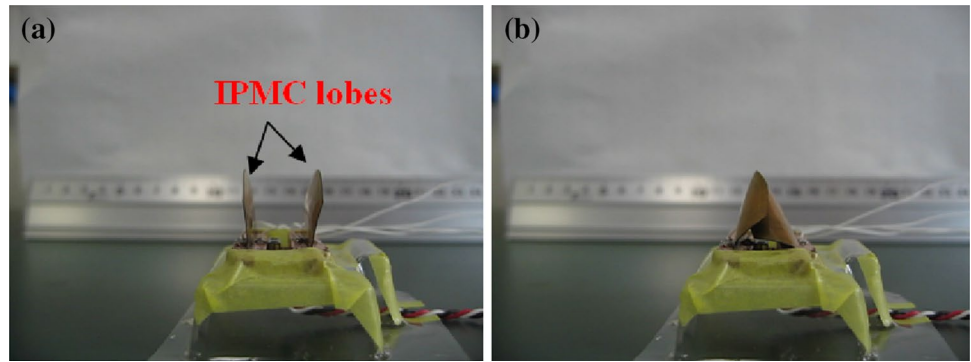
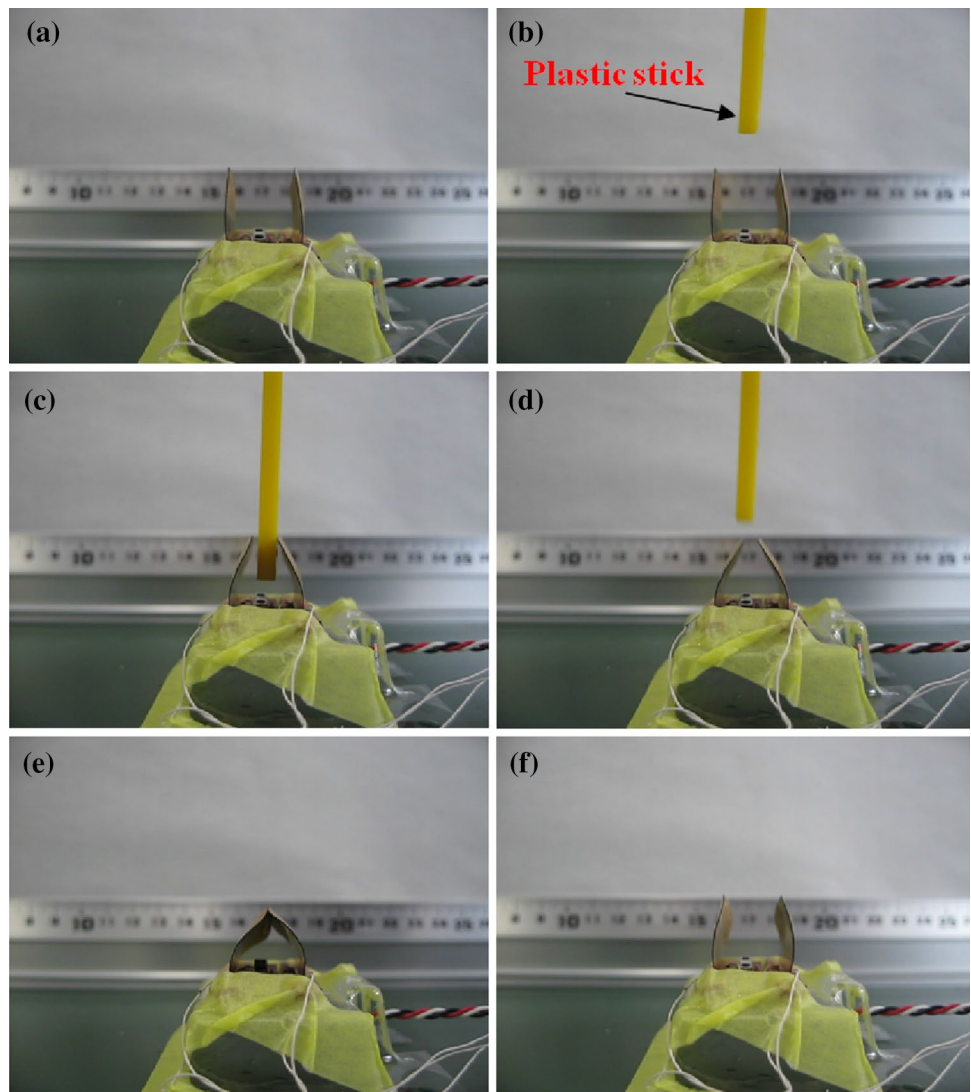


Fig. 9 Closing motion with a single proximity sensor: **a** initial state, **b** with a stick inserted, **c** with the stick detected, **d** with the stick withdrawn, **e** the lobes beginning to return, and **f** the final state



4.2 Grasping experiments

Figure 8 shows the closing motion, which was investigated to evaluate the maximum closing deformation of the two IPMC lobes (this is the motion that mimics the lobes of the

Venus flytrap). Figure 9 shows the closing motion using the proximity sensor to detect a moving stick. Initially, the two IPMC lobes were maintained open while no object was present between the two lobes. When the plastic stick was moved close to the proximity sensor, the two IPMC lobes

Fig. 10 Grasping ability measurements: **a** left view, **b** front view, and **c** grasping

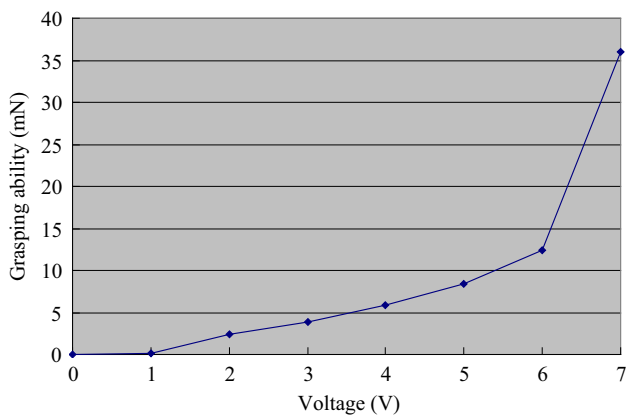
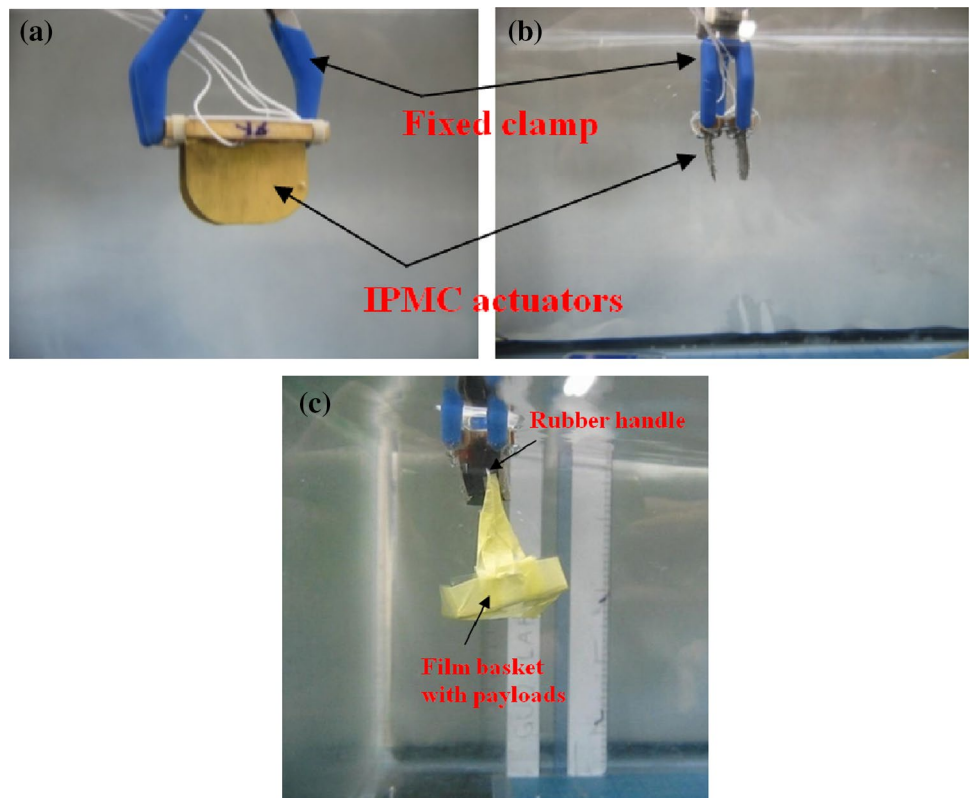


Fig. 11 Results of the grasping experiments

bent toward each other. When we moved the plastic stick away from the sensor, the two lobes opened.

4.3 Grasping ability

We conducted experiments to evaluate the grasping ability of the robot flytrap. Figure 10a and b show the fixed clamp used with the two IPMC lobes. The separation between the two lobes was 10 mm, and a rubber handle was used as the grasping part of a small basket, which was used to maintain a constant tip displacement between the two IPMC lobes.

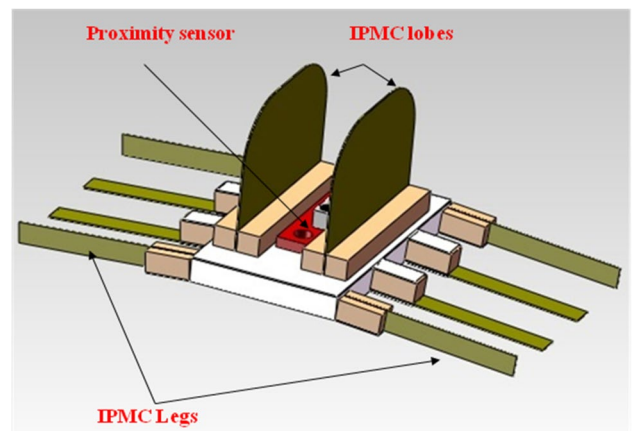


Fig. 12 The proposed structure of a movable robotic Venus flytrap

The static coefficient of friction μ_s between the IPMC and rubber handle was constant. Initially, the two IPMC lobes grasped the rubber handle of the small basket. More mass was then placed into the basket to gradually increase the payload. When the friction between the handle and the lobes was no longer able to support the payload, the small basket dropped. Figure 10c shows the grasping experiment.

We measured the maximum grasping payload with various applied voltages, as shown in Fig. 11. With a constant bending deformation, the grasping payload increased as the

voltage increased, exhibiting a similar trend to the results of the bending force measurements. The robotic flytrap was able to support a maximum payload of 36 mN with an applied voltage of 7 V.

5 Movable robotic flytrap

5.1 Structure

To enlarge the working area and reduce the number of required robotic flytraps, we added eight biomimetic IPMC legs to implement walking and rotating motion, as shown in Fig. 12. The eight actuators were all 14 mm long, 3 mm wide, and 220 μm thick. The total size of the microrobot was 33 mm in length, 58 mm in width, and 30 mm in height.

5.2 Walking and rotating mechanism

Figure 12 shows the distribution of the eight legs. The outer four vertical legs were used to drive the robot, and the inner four horizontal legs functioned as supporting members. The supporting legs bent downward to lift the body up, and the driving legs bent forward to generate a step. When the supporting legs bent upward, the driving legs then bent backward to move the body. The driving and supporting legs were driven at the same frequency, and the phase of the supporting legs lagged that of the driving legs by 90° (Shi et al. 2011). Figure 13 shows a single cycle of walking forward. By changing the bending direction of four driving legs between the two sides, the robotic Venus flytrap could walk forward or backward, as well as rotate clockwise and counter-clockwise.

6 Experiments

6.1 Prototype movable robotic flytrap

Figure 14 shows the prototype movable robotic flytrap. It was 33 mm long, 58 mm wide, and 30 mm high, and weighed 8.1 g. The IPMC actuator lobes measured $24 \times 18 \times 0.22 \text{ mm}^3$, the IPMC actuator legs measured

$24 \times 3 \times 0.22 \text{ mm}^3$, and the separation between the two IPMC lobes was 10 mm.

6.2 Walking and rotational motion

To evaluate walking locomotion, we carried out an experiment on an underwater plastic surface. We recorded the time to walk a distance of 100 mm using different applied signal frequencies with a voltage of 8 V. The experiment was repeated five times for each set of control signals to determine the average speed on the flat surface. Figure 15 shows that the walking speed was approximately proportional to the input voltage, and a top speed of 15 mm/s was obtained with a driving frequency of 3 Hz.

We also investigated the rotational motion on the same underwater plastic surface. We recorded the time to rotate through 90° with different frequency signals, and calculated the average angular velocity for five repetitions of the same experiment. Figure 16 shows that the angular velocity was approximately proportional to the input voltage, and a maximum rotational speed of 20.3°/s was obtained with a voltage of 8 V and a frequency of 3 Hz.

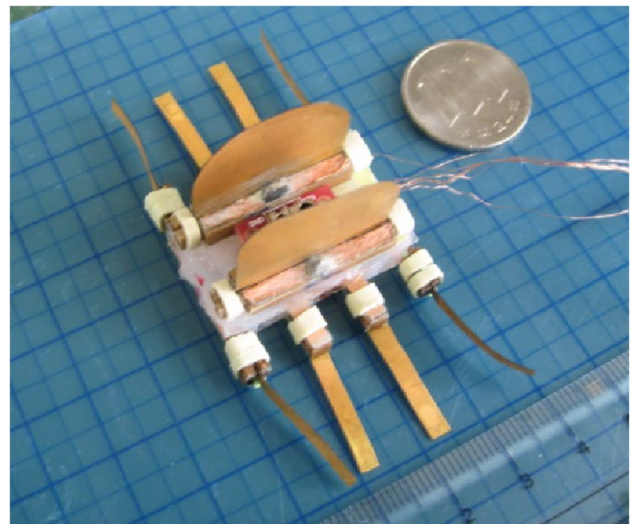


Fig. 14 The prototype movable robotic Venus flytrap

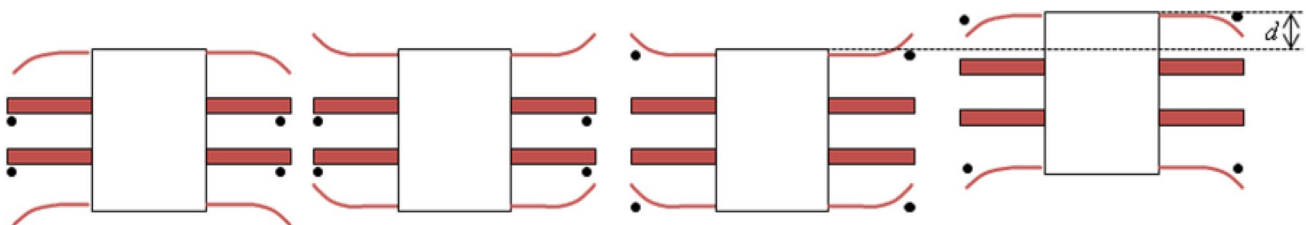


Fig. 13 A single cycle of walking forward. Dots indicate which legs were in contact the ground

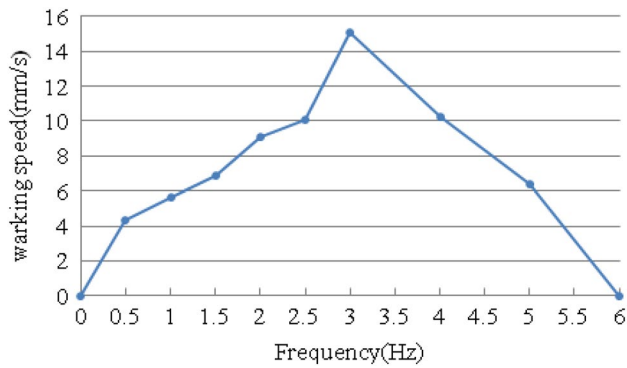


Fig. 15 Measured speed during walking

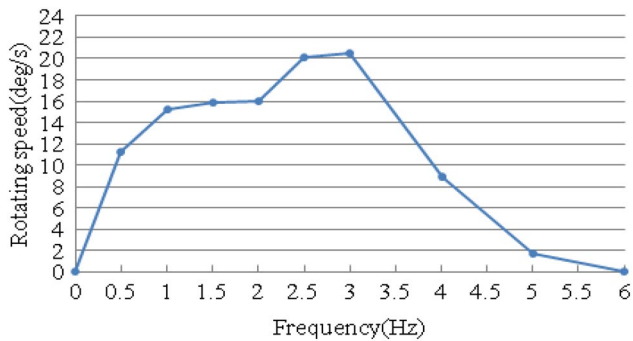


Fig. 16 Measured angular velocity during rotation

Fig. 17 Hybrid motion: **a** walking, **b** rotation, **c** walking, and **d** grasping

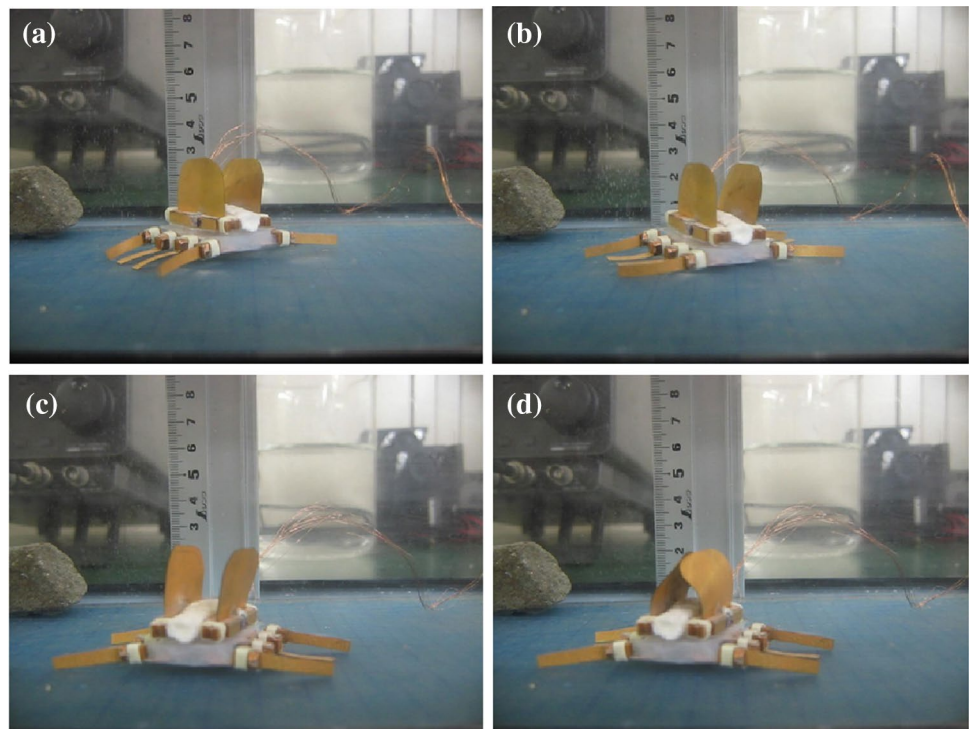


Figure 17 shows the hybrid motion of the robotic Venus flytrap. First, it walked forward to the desired location; second, it rotated by 45° ; third, it walked forward again to reach the working area; finally, the two IPMC lobes were bent in a grasping motion.

7 Improvements

We identified a number of areas for improvements to the prototype robotic flytrap. It was not straightforward to completely close the two lobes without gaps using a low voltage. We modified the robotic flytrap to improve the closing action, as shown in Fig. 18. We used three lobes to reduce the gaps. Furthermore, we used three proximity sensors to detect the location of the target (i.e., a fly) in the entire inner space of the lobes. We found that using three proximity sensors allowed more sensitivity than a single sensor.

Using this improved structure, we developed a prototype robotic flytrap with three IPMC lobes, as shown in Fig. 19, whereby the separation between lobes could be adjusted. This structure opened and closed like a flower, and could be carried by a walking microrobot to extend the working area. The resulting prototype robotic flytrap exhibited good performance, with potential applications as a toy or for use in an aquarium.

Fig. 18 Modified structure of the robotic flytrap

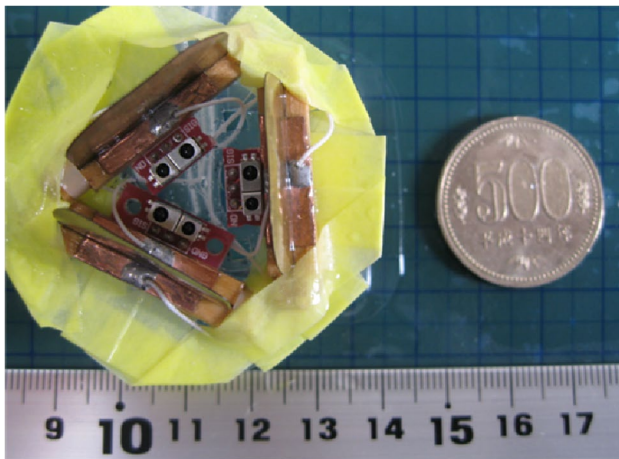
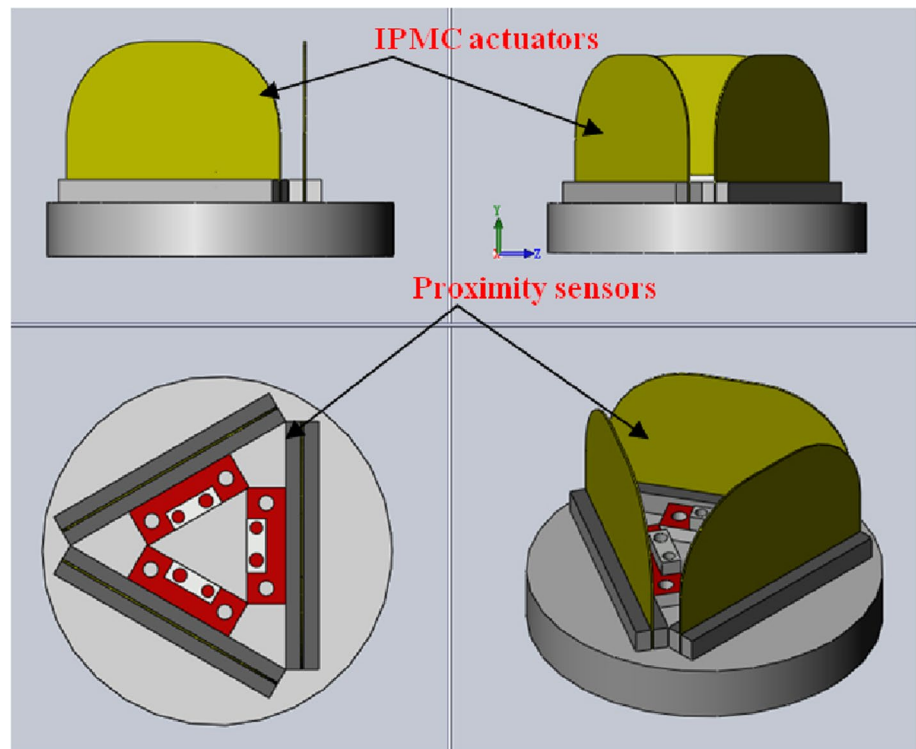


Fig. 19 Modified prototype robotic flytrap

8 Conclusions

We have described the design and development of a biomimetic robotic flytrap that was inspired by the Venus flytrap. The flytrap action was achieved using two ionic polymer metal composite (IPMC) actuators. First, we developed the structure of the robotic flytrap, and designed the control circuitry. We then evaluated the deformation and bending force generated by the IPMC lobes with various applied voltages. We developed a prototype robotic flytrap, and

carried out experiments using a single proximity sensor to imitate the trigger hairs of the Venus flytrap. To evaluate its grasping ability, we measured the maximum payloads that could be supported with various applied voltages: the robotic flytrap could hold a maximum payload of 36 mN with a voltage of 7 V.

To enlarge the working area, we integrated biomimetic walking and rotating motions, which we implemented using IPMC legs, to develop a prototype movable robotic flytrap, and evaluated its walking and rotational speeds. Finally, we improved the design of the robotic flytrap by using three IPMC lobes to eliminate the gaps between the lobes. Three proximity sensors were used to detect the location of the target.

As part of future work, the robotic flytrap could be carried by a larger robot, as described in our previous works, with potential applications in aquaria.

Acknowledgments This work was supported by the excellent young scholars Research Fund of Beijing Institute of Technology and the Basic Research Fund of the Beijing Institute of Technology (No. 3160012211405). This work was partly supported by National Natural Science Foundation of China (61375094).

References

- Behkam B, Sitti M (2006a) Design methodology for biomimetic propulsion of miniature swimming robots. *J Dyn Syst Measurement Control* 128(1):36–43

- Behkam B, Sitti M (2006b) Design methodology for biomimetic propulsion of miniature swimming robots. *J Dyn Syst Meas Control* 128:36–43
- Brunetto P, Fortuna L, Graziani S, Strazzeri S (2008) A model of ionic polymer–metal composite actuators in underwater operations. *J Smart Mater Struct* 17(2):025–029
- Chu W, Lee K, Song S, Han M, Lee J, Kim H, Kim M, Park Y, Cho K, Ahn S (2012) Review of biomimetic underwater robots using smart actuators. *Int J Precis Eng Manuf* 13:1281–1292
- Feng G, Liu K (2014) Fabrication and characterization of a micromachined swirl-shaped ionic polymer metal composite actuator with electrodes exhibiting asymmetric resistance. *Sensors* 14(5):8380–8397. doi:[10.3390/s140508380](https://doi.org/10.3390/s140508380)
- Guo S, Shi L, Xiao N, Asaka K (2012) A biomimetic underwater microrobot with multifunctional locomotion. *Robot Auton Syst* 60:1472–1483
- He Qingsong, Min Yu, Song Linlin, Ding Haitao, Zhang Xiaoqing, Dai Zhendong (2011) Experimental study and model analysis of the performance of IPMC membranes with various thickness. *J Bionic Eng* 8(1):77–85
- Heo S, Wiguna T, Park HC, Goo NS (2007) Effect of an artificial caudal fin on the performance of a biomimetic fish robot propelled by piezoelectric actuators. *J Bionic Eng* 4:151–158
- Jain PK, Datta S, Majumder S, Dutta A (2011) Two IPMC fingers based micro gripper for handling. *Int J Adv Robotic Syst* 8:1–9
- Kim B, Kim D, Jung J, Park J (2005) A biomimetic undulatory tadpole robot using ionic polymer-metal composite actuators. *Smart Mater Struct* 14:1579–1585
- Kim S, Tiwari R, Kim K (2011) A novel ionic polymer metal zno composite (IPMZC). *Sensors* 11(5):4674–4687. doi:[10.3390/s110504674](https://doi.org/10.3390/s110504674)
- Lee S, Kim K, Park I (2007) Modeling and experiment of a muscle-like linear actuator using an ionic polymer–metal composite and its actuation characteristics. *Smart Mater Struct* 16:583–588
- Lin Y, Yu C, Li C, Liu C, Chen J, Chu T, Su G (2014) An ionic-polymer-metallic composite actuator for reconfigurable antennas in mobile devices. *Sensors* 14(1):834–847. doi:[10.3390/s140100834](https://doi.org/10.3390/s140100834)
- Liu W, Jia X, Wang F, Jia Z (2010) An in-pipe wireless swimming microrobot driven by giant magnetostrictive thin. *Sens Actuators A Phys* 160(1):101–108
- Park I, Kim S, Kim D, Kim K (2007) The mechanical properties of ionic polymer-metal composites. *Proc SPIE*. doi:[10.1117/12.716670](https://doi.org/10.1117/12.716670)
- Shahinpoor M (2011) Biomimetic robotic Venus flytrap (*Dionaea muscipula* Ellis) made with ionic polymer metal composites. *Bioinspir Biomim* 6(4):046004, 1–11
- Shi L, Guo S, Asaka K (2011) Development of a new jellyfish-type underwater microrobot. *Int J Robot Autom* 26(2):229–241
- Shi L, Guo S, Asaka K (2012a) A novel jellyfish- and butterfly-inspired underwater microrobot with pectoral fins. *Int J Robot Autom* 27(3):276–286
- Shi L, Guo S, Li M, Mao S, Xiao N, Gao B, Song Z, Asaka K (2012b) A novel soft biomimetic microrobot with two motion attitudes. *Sensors* 12(12):16732–16758
- Shi L, Guo S, Kudo H, Asaka K (2012) Development of a Venus flytrap-inspired robotic flytrap, proceedings of 2012 IEEE International conference on robotics and biomimetics (ROBIO 2012), pp 551–556, Dec 11–14, Guangzhou, China
- Shi L, Guo S, Mao S, Li M, Asaka K (2013a) Development of a lobster-inspired underwater microrobot. *Int J Adv Rob Syst* 10(44):1–15. doi:[10.5772/54868](https://doi.org/10.5772/54868)
- Shi LW, He YL, Guo SX, Kudo H, Li MX, Asaka K (2013) IPMC actuator-based a movable robotic Venus flytrap, proceedings of 2013 ICME international conference on complex medical engineering (ICME CME 2013), pp 375–378, May 25–28, Beijing, China
- Villanueva A, Joshi K, Blottman J, Priya S (2010) A bio-inspired shape memory alloy composite (BISMALC) actuator. *Smart Mater Struct* 19(025013):1–17
- Villanueva A, Smith C, Priya S (2011) A biomimetic robotic jellyfish (Robojelly) actuated by shape memory alloy composite actuators. *Bioinspir Biomim* 6(3): 036004, 1–16
- Wang Z, Hang G, Li J, Wang Y, Xiao K (2008) A micro-robot fish with embedded SMA wire actuated flexible biomimetic fin. *J Sens Actuators A Phys* 144(2):354–360
- Wei H, Su G (2012) Design and fabrication of a large-stroke deformable mirror using a gear-shape ionic-conductive polymer metal composite. *Sensors* 12(8):11100–11112. doi:[10.3390/s120811100](https://doi.org/10.3390/s120811100)
- Yeom S, Oh I (2009) A biomimetic jellyfish robot based on ionic polymer metal composite actuators. *J Smart Mater Struct* 18(085002):1–16
- Yim W, Lee J, Kim KJ (2007) An artificial muscle actuator for biomimetic underwater propulsors. *Bioinspir Biomim* 2:S31–S41
- Zhang W, Guo S, Asaka K (2006) A new type of hybrid fish-like microrobot. *Int J Robot Autom Computing* 3(4):358–365
- Zhou Y, Chiu C-W, Sanchez CJ, González JM, Epstein B, Rhodes D, Vinson SB, Liang H (2013) Sound modulation in singing katydids using ionic polymer-metal composites (IPMCs). *J Bionic Eng* 10(4):464–468